Ground mobile observation system for measuring multisurface microwave emissivity

Wenying He [1,2,*] Hongbin Chen[1,2,*] Yuejian Xuan[1] Jun Li[1]
Minzheng Duan[1,2] Weidong Nan [1,3]
1.Key Laboratory of Middle Atmosphere and Global Environment Observation, Institute of Atmospheric Physics, Chinese Academy of Sciences, Beijing 100029, China
2.University of Chinese Academy of Sciences, Beijing 100049, China
3 Xianghe Observatory of Whole Atmosphere, Institute of Atmospheric Physics, Chinese Academy of Sciences, Xianghe 065400, China

Abstract

Large microwave surface emissivities with a highly heterogeneous distribution and the relatively small hydrometeor signal over land make it challenging to use satellite microwave data to retrieve precipitation and to be assimilated into numerical models. To better understand the microwave emissivity over land surfaces, we designed and established a ground observation system for the in situ observation of microwave emissivities over several typical surfaces. The major components of the system include a dual-frequency polarized ground microwave radiometer, a mobile observation platform, and auxiliary sensors to measure the surface temperature and soil temperature and moisture; moreover, observation fields are designed comprising five different land surfaces.

Based on the observed data from the mobile system, we preliminarily investigated the variations in the surface microwave emissivity over different land surfaces. The results show that the horizontally polarized emissivity is more sensitive to land surface variability than is the vertically polarized emissivity: the former decreases to

* Corresponding author E-mail addresses: hwy@mail.iap.ac.cn (Wenying He)
* Corresponding author E-mail addresses: chb@mail.iap.ac.cn (Hongbin Chen)

0.75 over cement and increases to 0.90 over sand and bare soil and up to 0.97 over grass. The corresponding emissivity polarization difference is obvious over water (>0.3) and cement (approximately 0.25) but reduces to 0.1 over sand and 0.05 over bare soil and almost 0.01 or close to zero over grass; this trend is similar to that of the Tb polarization difference. At different elevation angles, the horizontally/vertically polarized emissivities over land surfaces obviously increase/slightly decrease with increasing elevation angles but exhibit the opposite trend over water.

Key words: Ground mobile observation system, microwave radiometer, microwave surface emissivity, surface temperature, land surface

1 Introduction

The land surface microwave emissivity varies but is generally high (~ 0.90) and thus generates strong surface radiance; however, this strong surface radiance obscures radiance from the atmosphere and hydrometeors, making it more difficult to assimilate and precisely retrieve atmospheric parameters using satellite microwave data over land (McNally et al., 2000; Farbou et al., 2005; Schwartz et al., 2012). Moreover, due to complex variations affected by many surface factors, such as soil type, wetness, vegetation type and surface roughness, the land surface emissivity is poorly understood. Hence, the land surface microwave emissivity constitutes a major parameter limiting the application of spaceborne microwave data over land.

Microwave emissivity models have been developed only for a limited range of frequencies and surface conditions. For example, the emissivity over bare soil was modeled at lower frequencies, and the soil dielectric constants were obtained from

ground-based measurements (Wang and Schmugge, 1980). The emissivity over the vegetation canopy was simulated using a radiative transfer model with a large number of canopy optical parameters (Mo and Schmugge, 1987; Isaacs et al., 1989; Fung, 1994). Weng (2001) developed a microwave land emissivity model to quantify the emissivity over various surface conditions, including snow, deserts, and vegetation. Xie et al. (2017) developed a parameterized soil surface emissivity model for bare soil surfaces and compared with Weng's model, results reflected the reduced overall errors, especially for horizontal polarization. Ultimately, the microwave emissivity of land surfaces is determined mainly by the soil dielectric constant, which is influenced by the physical temperature, soil texture and moisture content, and vegetation structure and type. As a result of these complicated parameters with numerous uncertainties, establishing a common physical emissivity model and accurately obtaining emissivity estimates by using only an emissivity model remain challenging.

Satellite observations offering extensive coverage have been used to estimate the regional and global distributions of land surface emissivity since the 1990s (Prigent et al., 2000; Moncet et al., 2011). To avoid the impacts of the complex variability of clouds and precipitation in the atmosphere, only the brightness temperatures observed by spaceborne microwave instruments under clear sky conditions are generally selected to calculate the land surface microwave emissivity. Jones and Vonder Haar (1997) used SSM/I (Special Sensor Microwave Imager) microwave observations and GOES/VISSR (Geostationary Operational Environmental Satellite/Visible Infrared Spin-Scan Radiometer) infrared data that were closely matched in both space and time

to retrieve the microwave land emissivity over the Central United States and utilized the infrared data with a constant infrared emissivity of 0.98 to calculate the land skin temperature (LST) under clear sky conditions. Further, Ruston and Vonder Haar (2004) directly employed spatially varying infrared surface emissivities in the retrieval of LST to calculate the microwave emissivity and discovered that the atmospheric-corrected microwave surface emissivity is valuable for determining land surface characteristics but is sensitive to rain events. Prigent et al. (1997, 1999) calculated the land surface microwave emissivity over Africa, some parts of Europe and West Asia by combining SSM/I data with LST observations provided by ISCCP (International Satellite Cloud Climatology Project). With subsequently improved ISCCP LST and cloud product data, Prigent et al. (2006) presented a global land surface microwave emissivity database retrieved from 10 years of SSM/I data and plotted the monthly average land surface microwave emissivity onto a geographic map. In their work, the microwave emissivity retrieval was based primarily on radiative transfer calculations, in which infrared data were used to determine the LST under clear sky conditions, and atmospheric sounding data were used to take the effects of atmospheric attenuation into account. Nevertheless, due to the complexity and variability of clouds and atmospheric precipitation, land surface microwave emissivity estimates derived from satellite observations are available only under clear sky conditions. Moreover, the cloud screening and LST retrieval methods still contain numerous uncertainties, which represent the main sources of errors in emissivity calculations.

At present, the accuracy of surface emissivity estimates calculated from either emissivity models or satellite observations is limited by the complexity of the land surface and the variability of vegetation types and soil moisture. Another important limitation is availability and accuracy of necessary input parameters on a global scale. Hence, surface emissivity calculations need to be verified and improved with more in situ observation data.

To better understand the variation characteristics of surface emissivity with surface conditions, Ulaby et al. (1985) combined field experiments and theoretical research and revealed that the land surface microwave specific emissivity is strongly correlated with the distributions of soil moisture and vegetation. In addition, a few observation experiments using ground-based microwave radiometers have been carried out since the 1990s to study the variation characteristics of emissivity over different surfaces (Njoku and O'Neill,1982; Matzler, 1990, 1994; Calvet, 1997; Wigneron, 1994; Morland et al., 1995). More recently, in situ passive microwave radiometer measurements over snow cover and sub-Arctic frozen soil have been used to validate empirical emission models (Lemmetyinen et al., 2015; Montpetit et al., 2018). Additionally, an aircraft-flown microwave radiometer was used to directly observe the surface emissivity over forests, crops, snow and ice to analyze the sensitivity of those emissivities to the view angle, frequency, measurement time and surface characteristics (Hewison, 2001; Wigneron et al., 1997; Hewison and English, 1999).

The observation mode of a microwave radiometer in a field experiment is an

important consideration. Usually, ground-based radiometers are fixed when scanning the observed field; for example, they can be mounted on a truck or a tower (Matzler, 1990; Lemmetyinen et al., 2015), allowing the instrument to better determine the temporal evolution of surface emissivity over single type of land-cover area. In contrast, using a mobile mode, such as airborne and mobile sled-based radiometers (Morland, 2003; Lemmetyinen et al., 2015; Montpetit et al., 2018), can better reveal the spatial evolution of surface emissivity over different land-cover areas, but it is not easy to obtain long-term emissivity observations due to the high cost and effort.

To obtain the long-term temporal evolution of surface emissivity over different types of surfaces simultaneously, we proposed and developed a ground mobile observation system to enhance in situ microwave emissivity observations. Long-term continuous emissivity field experiments can help to more accurately understand the characteristics of passive microwave polarized emissivities over typical land surfaces, form a benchmark for verifying the retrieved emissivities from satellite or emission models, and establish an emissivity parameterization scheme for a given surface in radiance assimilation. The outline of this paper is as follows: the design of the ground mobile observation system for measuring surface emissivity is introduced in section 2; data and method used for the emissivity calculations are described in section 3; the surface emissivity estimates obtained directly from the observation system are discussed preliminarily in section 4; and a final short summary is given in section 5.

2. Ground mobile observation system for surface microwave emissivity

To obtain the surface emissivity over several typical surfaces simultaneously, we

designed a ground mobile observation system to carry out long-term field experiments over 5 test plots. Fig. 1 is an on-site photo of the observation system operating at the Xianghe observation site (116.98° E, 39.76° N), Hebei Province, China. As shown in Fig. 1, the mobile observation system consists of five main parts: a dual-frequency (18.7 and 36.5 GHz), dual-polarized ground-based microwave radiometer to observe the surface and sky radiances, a mobile platform to move back and forth along a track, and three auxiliary sensors to measure the surface temperature, soil temperature and moisture. The observation field includes five test plots, namely, water, cement, sand, bare soil and grass. From the observation system, we can directly obtain surface microwave emissivity estimates more accurately than is possible from satellite data or emissivity models, which is important to properly understand the variation characteristics of land microwave emissivities and to improve the emissivity parameterization schemes used in models.

Fig 1 On-site photo of the surface microwave emissivity observation system operating over various surfaces at the Xianghe site, China

2.1 Ground-based microwave radiometer

The core device of the observation system is a dual-frequency (18.7 and 36.5 GHz), dual-polarized (horizontal and vertical) microwave radiometer (RPG-4CH-DP) produced by Radiometer Physics GmbH, Germany. The RPG-4CH-DP radiometer is a high-performance instrument with a direct detection receiver and a completely automatic calibration system. The radiometer is mounted on an accurate elevation/azimuth positioner so that the whole system can perform scans in any direction from the sky to the ground, thereby realizing complex scanning schemes, such as all-sky monitoring and all-round monitoring of the ground. The RPG-4CH-DP can distinguish cloud/raindrop particles during precipitation and monitor soil moisture and vegetation parameters by using signals with different polarizations. Both frequencies of 18.7 GHz and 36.5 GHz have been widely combined to detect snow depth and snow water content and are frequently used in most spaceborne microwave imagers, such as the SSM/I, AMSR-E (Advanced Microwave Scanning Radiometer for EOS) and GMI (GPM Microwave Imager) sensors. The directly observed surface emissivities at these two frequencies can provide highly accurate references for the verification and assimilation of spaceborne microwave observations.

The RPG-4CH-DP radiometer has a comparable half-power beam width of approximately 6° and a calibration accuracy of ±1 K. Currently, the height of the instrument above the ground is 2.5 m, which results in a half-power footprint width of 0.22 m on average. More details regarding the instrument specifications for the RPG-4CH-DP are shown in Table 1.

Table 1 Instrument Specifications

Parameter	Specification
Radiometric resolution	0.2 K RMS (1.0 s integration time)
Optical resolution	HPBW: 6.0° (Sidelobe level <-30 dBc)
Absolute system stability	1.0 K
Receiver and antenna thermal stabilization	Accuracy <0.05 K
Pointing speed	Elevation: 3°/sec, azimuth: 5°/sec
Radiometric range	0-350 K
Operating temperature range	-40°C to +45°C
Power consumption	<350 watts on average, 500-watt peak
Weight	105 kg for receiver modules, 300 kg for positioner

Currently, the RPG-4CH-DP provides only the basic brightness temperature (Tb) data in 4 channels without other related products. By incorporating the auxiliary observations from the observation system, we broadened the application of the instrument, denoted RPG-XCH-DP, thereby providing not only the basic microwave radiance but also the complex surface emissivity.

2.2 Mobile system (platform)

The multitarget mobile system comprises a track, a mobile platform, a driving system and a control unit. As the sketch of the mobile system in Fig. 2 shows, the 25 m track is parallel to the test plots with an observation interval of 0.3 m. The mobile platform placed on the track is a metal box 4 m in length, 0.8 m in height, and 1.0 m in depth. The driving system includes a stepper motor, transmission mechanism, and communication cable connected to the mobile platform and power supply. The control unit consists of a single-chip microcomputer, timer and stepper motor driver, which can set the moving time and control the operation of the driving device. The control device is installed on the mobile platform and connects both driving devices.

In this experiment, to obtain the microwave emissivity over different surfaces in near-simultaneous time, the RPG-4CH-DP is mounted on the mobile platform and moves back and forth along the track. The communication system for receiving the data and the power supply are placed in the metal box. According to the commands

from the single-chip microcomputer and the driving force from the stepper motor, the mobile platform moves along the track similar to a small train, and the onboard radiometer scans the 5 test plots at fixed times every day.

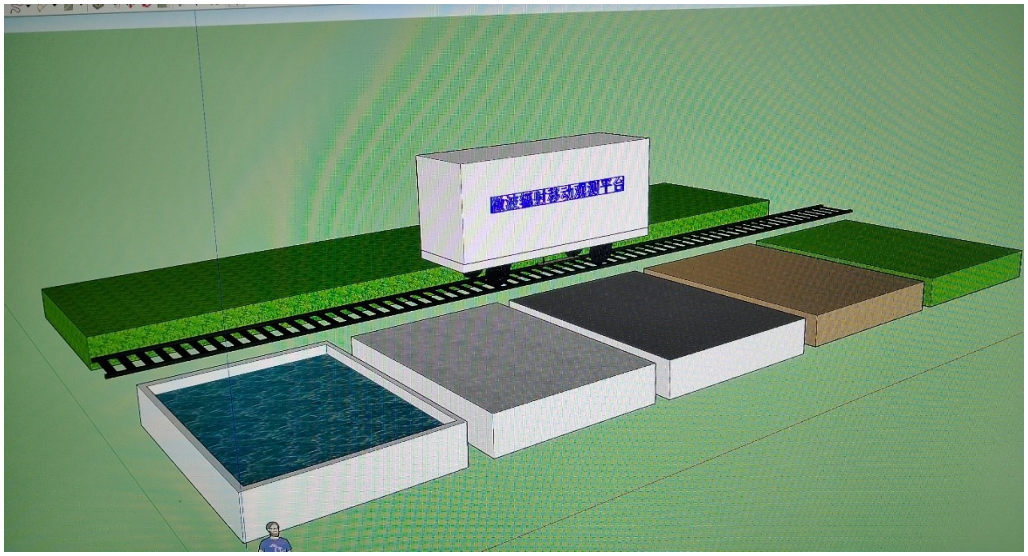

Fig. 2 Sketch of the mobile platform

2.3 Observation field and auxiliary data

Fig. 3 shows a sketch of the observation field, including the 5 test plots distributed along the 25 m track. Currently, 5 surface types are considered in the observation field, namely, water, cement, sand, soil and grass. For the water body, a plastic pool 6 m long and 2.4 m wide is used to hold the water. The adjacent cement surface consists of a 2 m wide footpath. The remaining three plots of sand, bare soil and grass are the same size (approximately 6 m long by 4 m wide) and are separated by a distance of approximately 2 m.

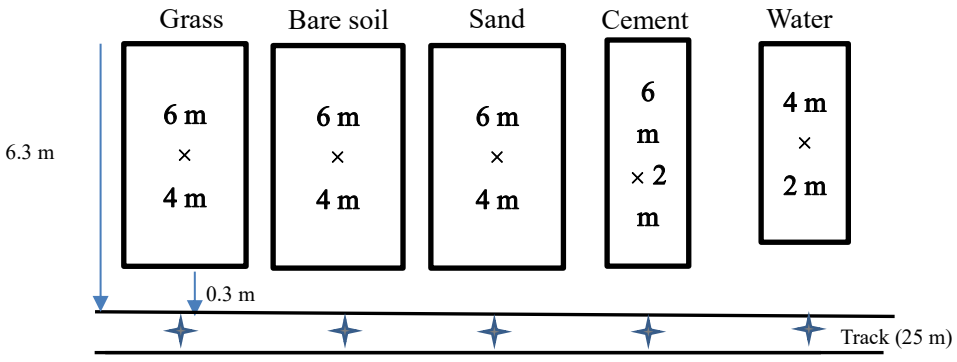

Fig. 3 Sketch of the observation field (including 5 test plots: water, cement, sand, bare soil and grass), where ✦ denotes the position of a touching switch

To scan each plot at the same place at a fixed time, five touching switches corresponding to the center of each plot are fixed on the track to stop the moving platform so that the radiometer can scan the same place for a couple of minutes. By using this mobile platform, the ground-based radiometer can scan multiple surfaces almost simultaneously (i.e., within 1 hr), thereby providing valuable measurements for understanding the variation in surface emissivity over different land surfaces with different characteristics.

The auxiliary data include mainly the surface temperature, soil temperature and soil moisture. Five thermometers with a PT100 temperature sensor made by Honeywell company are placed separately on each test plot to measure their surface temperature. In addition, an SI-111 precision infrared radiometer developed by Apogee Instruments Inc. is fixed on a stand of the RPG-4CH-DP radiometer to obtain the surface temperature of each plot while the microwave radiometer is moving. Furthermore, a set of soil temperature and moisture sensors is fixed at three soil depths, 5 cm, 10 cm and 20 cm, to detect the subsurface soil temperature and humidity. To monitor the real-time working situation of the whole observation system, a digital video camera is installed near the field to record the states of the mobile platform and radiometer as well as changes in the weather, such as the presence of cloud cover, rain or snow.

2.4 Scanning mode

To directly obtain the surface emissivity, a combined mode of ground observations at multiple elevation angles and zenith observations is designed, in which the former monitors mainly the surface radiance while the latter monitors the sky radiance in the same 1 hr period.

The ground observation mode is illustrated in Fig. 4. The mobile platform is triggered every hour, and the microwave radiometer operates using the ground scanning mode at this time. The scan is performed from the horizon (0°) to the ground, and the elevation angle is defined as the angle between the scanning direction and the horizontal. A negative value indicates an angle below the horizon, which is equivalent

to 90°-θ, where θ is the incident angle, an important parameter for describing spaceborne radiometer scanning. The radiometer is 2.5 m above the ground, so it can

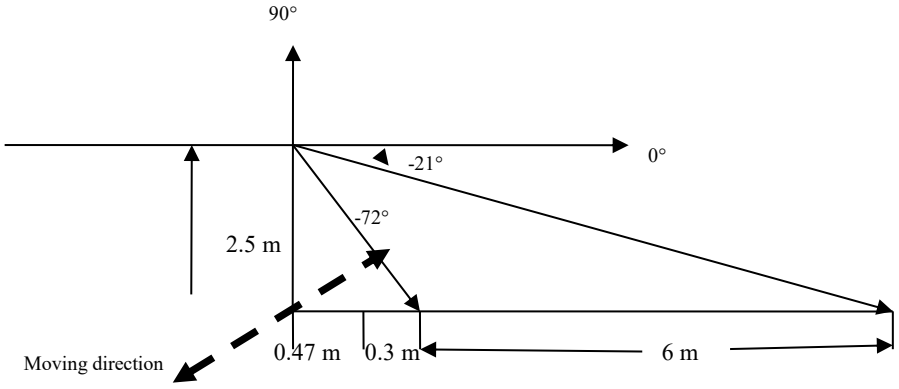

Fig. 4 Sketch of the combined scanning mode of the microwave radiometer

scan each test plot with a length of 6 m when the elevation angle is between -21° and -72°, as shown in Fig. 4. The valid elevation angle range for water is different due to the different length of the pool. To determine the surface emissivity variation with the elevation angle, the radiometer is set to scan each test plot with an angle interval of 3° from -21° to -45°, an angle interval of 5° from -45° to -70°, and then back to -21° to scan the test plot repeatedly during the ground observation mode. To acquire ground observations over all 5 test plots within 1 hr, each plot is given 9 minutes; in other words, the mobile platform will move to the cement plot at 9 min, the sand plot at 18 min, the bare soil plot at 27 min, and finally the grass plot at 36 min. After finishing the ground observations in all 5 test plots, the mobile platform will begin to move back at 45 min and reach the beginning location after approximately 6 min. During the return trip, the scan mode changes to the zenith observation mode so that the radiometer scans from the ground to the sky. When the elevation angle is raised to 90°, the radiometer will continually acquire zenith observations for approximately 5 min to obtain the sky radiance. After obtaining these zenith observations, the elevation angle changes from the zenith observation mode to the ground observation mode at -21° so that the radiometer is already in the ground observation mode when the next measurement cycle arrives. In this way, the radiometer on the mobile platform can obtain not only the ground radiance over 5 test plots but also the sky radiance within a

1 hr period. Here, we assume that 1 hr is short enough to neglect the minute-scale differences in the surface and sky radiance, and thus, the mobile system can obtain the microwave emissivity over different surfaces nearly simultaneously.

3 Data and method

Three types of observation data are obtained from the field experiment: the microwave brightness temperature (Tb) at different scanning angles from the ground microwave radiometer; the surface temperature (Ts) of the five test plots measured from the ground thermometers and infrared sensor; and the soil temperature and moisture at three depths in the sand and bare soil plots.

When ground microwave radiometer scans the surface, the measured Tb comes mainly from two contributions: that of upward radiation from the surface and that of the reflected downward atmospheric radiance. Thus, the measured Tb can be approximately expressed by Eq. (1):

$$T_b = \varepsilon T_s + (1-\varepsilon) T_{sky} \quad (1)$$

where ε is the surface emissivity, T_s is the surface temperature, and T_{sky} is the radiance from the sky. From Eq. (1), the surface emissivity can be directly calculated using Eq. (2) by combining the Tb contributions from the surface and sky with the surface temperature synchronously measured from the infrared sensor in the observation system.

$$\varepsilon = (T_b - T_{sky})/(T_s - T_{sky}) \quad (2)$$

It is noted here that Eq.(1) is assumed for specular reflection, and was used in previous similar observation studies (Lemmetyinen et al., 2015; Montpetit et al., 2018), so we used Eq.(1) and (2) to calculate surface emissivity in this work. The dual-polarized radiometer can provide both vertical and horizonal polarization information, then the ideal and uniform Lambertian surface is too simple and the bidirectional reflectance (BRDF) surface seems more complex, and the specular reflection is a good option. The results derived from this assumption will be further investigated by combining more auxiliary observations in the actual surface of test plots.

Through applying the ground mobile observation system for surface microwave emissivity and combining the video camera records with the soil temperature and moisture measurements, we can not only directly obtain highly accurate surface microwave emissivity observations over different test plots but also investigate the variation characteristics of the surface emissivity under different weather conditions.

4. Preliminary results

Considering both the viewing field of the microwave radiometer and the size of the test plots, the elevation angle range between -24° and -65° is chosen for observing the land test plots (cement, sand, soil and grass), while elevation angles between -33° and -65° are valid for observing the water surface. Here, we focus on the variations in the radiance and surface emissivity over the 5 test plots during the observations recorded in October 2018 under clear sky conditions.

4.1 Radiance

Since a scanning angle of 36° is equivalent to an incident angle of 54° used for many spaceborne microwave imagers, such as AMSR-E (55°) or SSM/I (53°), we first compare the variation in the observed Tb over different surfaces at an elevation angle of 36°. As Fig.5a shows, the changes in the observed Tb at 36.5 GHz in horizontal (Tb36h) and vertical (Tb36v) polarization over the four land surfaces within 24 hr (Beijing Time, BJT) are quite similar, with smaller values at night and larger values at noon. Less variation in the radiance is noted at Tb36v (not shown), but more significant variations are detected at Tb36h over the four surfaces (Fig. 5a): the observed Tb36h from grass is approximately 270-285 K but varies within 240-270 K over sand and bare soil and reaches only 200-230 K for cement. The observed Tb at

18.75 GHz within 24 h shows similar variations with only slight changes among the different land surfaces. Likewise, the corresponding polarization differences (V-H) of Tb within 24 hr are very similar to one another, so both DTb18vh and DTb36vh at 02:00 (BJT) are shown in Fig. 5b, revealing a slight difference (close to zero) for grass but considerably larger differences for water and cement (almost up to 70 K for water) and smaller differences over sand and soil (below 30 K). In addition, the values of DTb18vh are larger than those of DTb36vh. The Tb polarization difference is more significant over water than over land and is closely related to the roughness of the land surface. In addition, the roughness of grass is obviously larger than that of the other three land surfaces and thus scatters more surface radiance and reduces the polarization difference. Therefore, the observed Tb polarization differences over the different surfaces shown in Fig. 5b appear reasonable, and the given quantitative polarization differences for certain surfaces can serve as a valid reference for identifying land surfaces and water bodies.

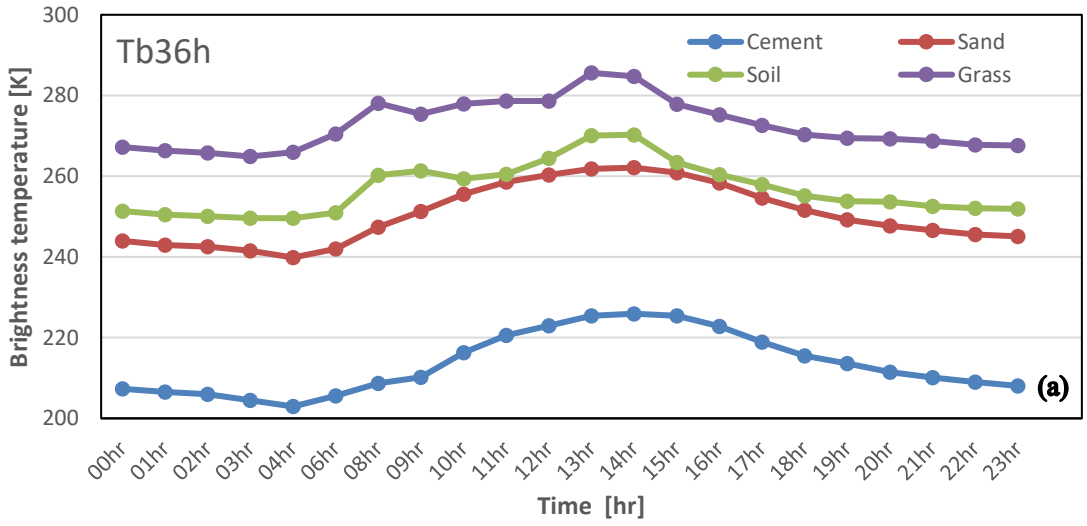

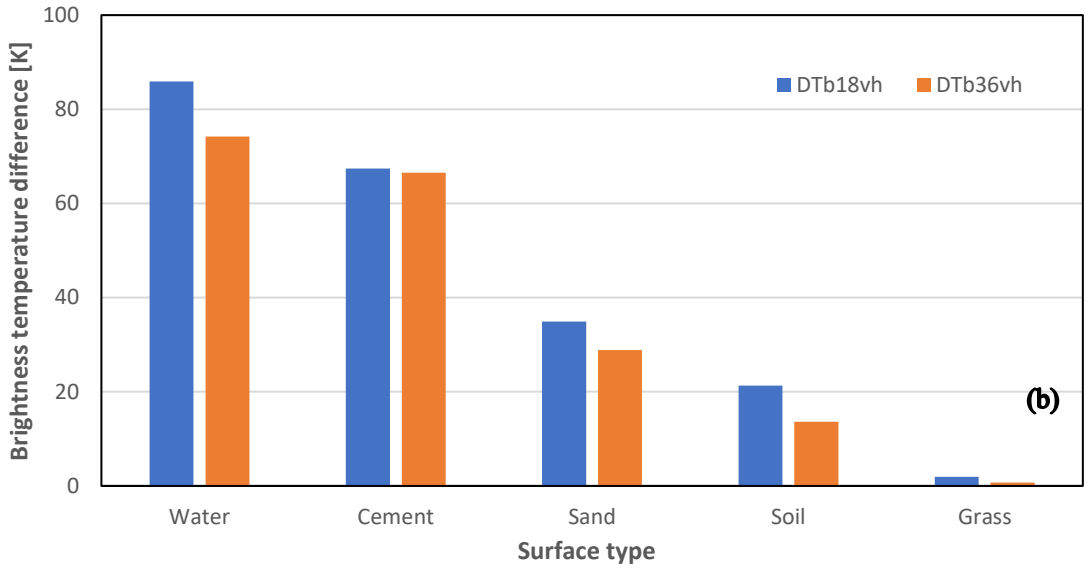

Fig. 5 Variations in the observed Tb (a) and Tb polarization differences (b) over different surfaces in October 2018.

To study the variations in Tb at more than a single angle, Fig. 6a shows the changes in the observed Tb with the elevation angle ranging from 24° to 65° over the four land surfaces. The horizontally polarized Tb is clearly more sensitive to the land surface type than the vertically polarized Tb with increasing elevation angle; in particular, Tb36h rises rapidly from 180 K to 240 K over cement but slowly increases from 240 K to 260 K over sand and bare soil and remains almost constant over grass. In contrast, the variations in the vertically polarized Tb with increasing elevation angle are similar among the land surfaces and are smaller than those in the horizontally polarized Tb, showing a decreasing trend from 280 K to 260 K over different surfaces. The variations in the observed Tb over water are presented in Fig. 6b. Different from the above observations over land surfaces, the vertically polarized Tb over water obviously reduces from 200 K to 140 K with increasing elevation angle, while the horizontally polarized Tb slowly rises from 100 K to 120 K, almost opposite

353 to the Tb polarization variations over land surfaces. The corresponding changes in the
354 polarization difference of Tb at 18.75 GHz (DTb18vh=Tb18v-Tb18h) over all 5
355 classes of surfaces are further plotted in Fig. 6c. In general, the Tb polarization
356 difference decreases with increasing elevation angle, and the variated ranges with the
357 elevation angle over the 5 classes surfaces in Fig. 6c are similar to those in Fig.5b;
358 thus, the decreasing trend is most obvious over water and cement and lest evident
359 over grass with increasing elevation angle. The variations of the Tb polarization
360 difference at 36.5 GHz with the elevation angle are similar to those at 18.75 GHz over
361 all 5 test plots.

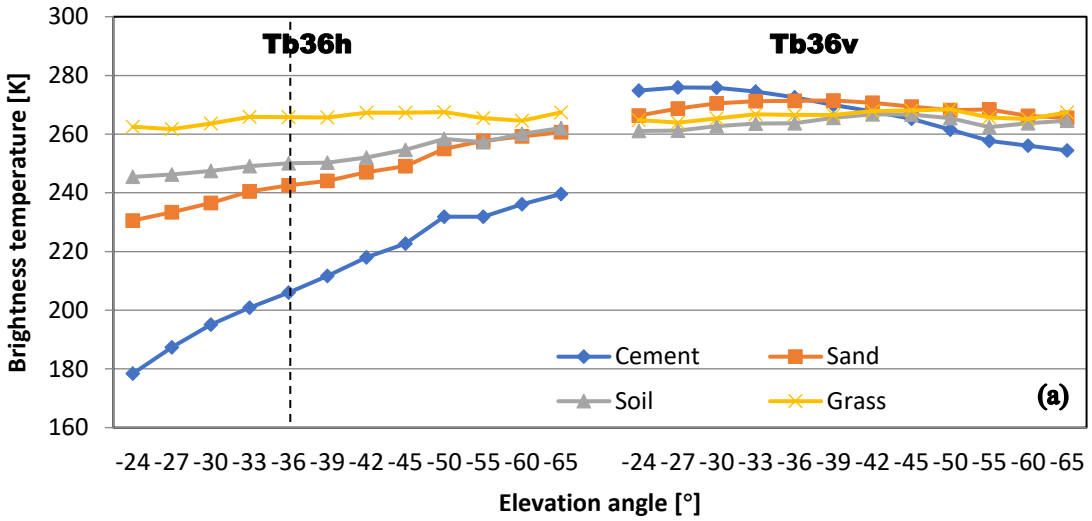

362

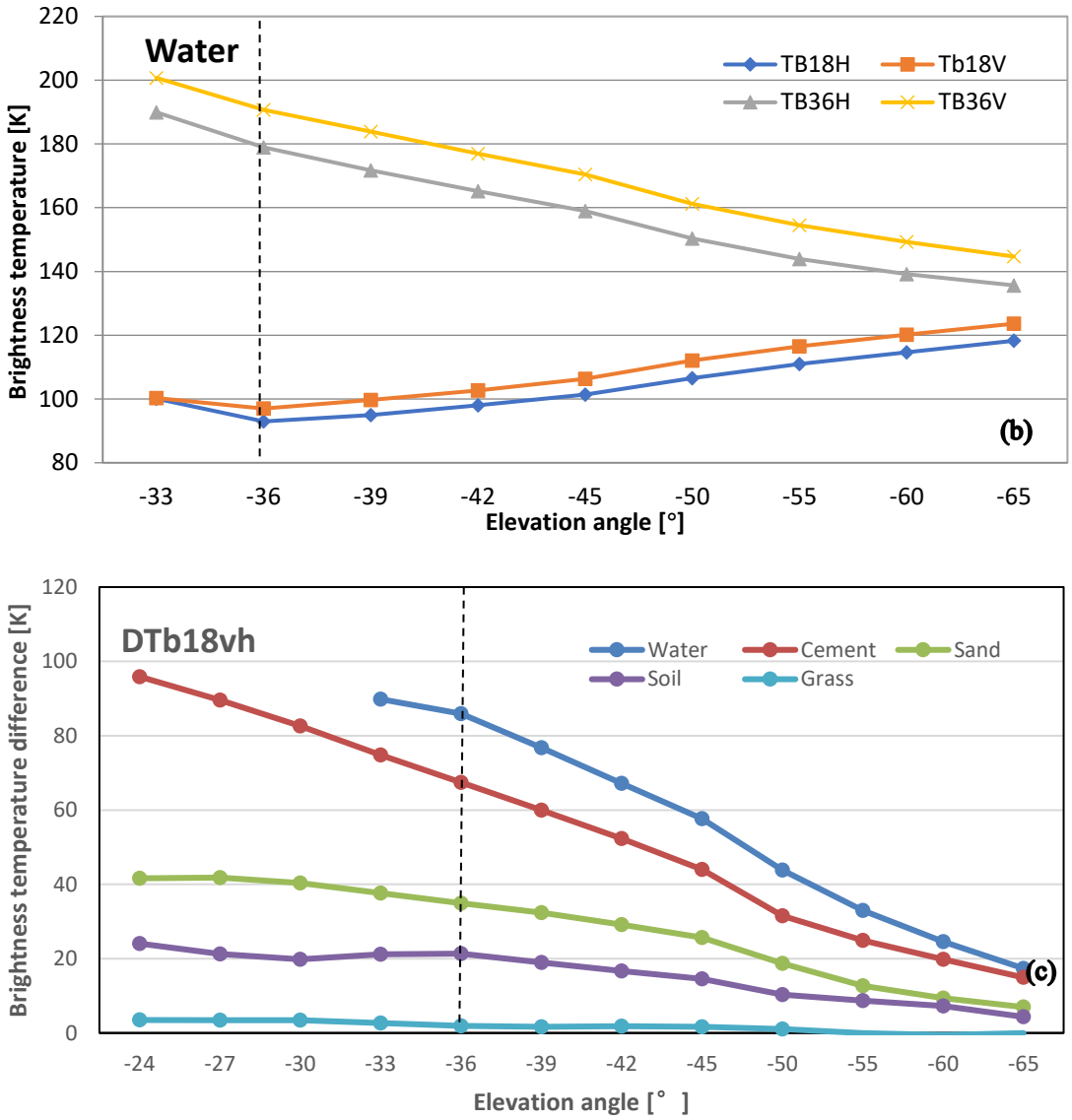

Fig. 6 Variations in the observed Tb over different land surfaces(a) and water surface(b) as well as Tb polarized difference(c) with the elevation angle in Oct. 2018. The vertical dotted line corresponds to elevation angle 36°

4.2 Surface microwave emissivity

Combining the surface and sky Tb radiance with the surface temperature derived from the infrared sensor, the surface emissivity (ε) is derived from Eq. (2). Since the diurnal variation of ε is more constant and less significant than that of the Tb radiance, the surface emissivity observed at 02:00 (BJT) is chosen for the

following investigation. First, the polarized ε at both 18.75 and 36.5 GHz and their polarization differences at an elevation angle of 36° are compared in Fig. 7a. The vertically polarized ε (ε_v) is clearly much larger than the horizontally polarized ε (ε_h), and the ε values at the same frequencies are close, but the ε values over water is smaller than those over the four land surfaces due to quite different dielectric constant. The ε_h values obviously differ among the 4 land surfaces, although their corresponding ε_v values are relatively similar, exceeding 0.95, which indicates that ε_h is more sensitive to land surface variability than ε_v. The ε_h is lower than 0.75 over cement but increases to 0.90 over sand and bare soil and up to 0.97 over grass. Thus, the emissivity polarization difference (ε_v-ε_h) shown in Fig. 7b is obvious over water (>0.3) and cement (approximately 0.25) but reduces to 0.1 over sand and 0.05 over bare soil and almost 0.01 or close to zero over grass; this trend is similar to that of the Tb polarization difference shown in Fig. 5b. Emissivity polarization difference is more significant over water than over land due to different surface reflectivity and dielectric constant properties. Among four land surfaces ε_v-ε_h over cement is most obvious and over grass is slight, which is closely related to land surface roughness. Both Tb and emissivity polarized difference demonstrated that surface roughness over grass is obviously larger than that over other three land surfaces, especially smooth cement surface, thus generate more volume scattering by vegetation and weakens the polarization difference over grass.

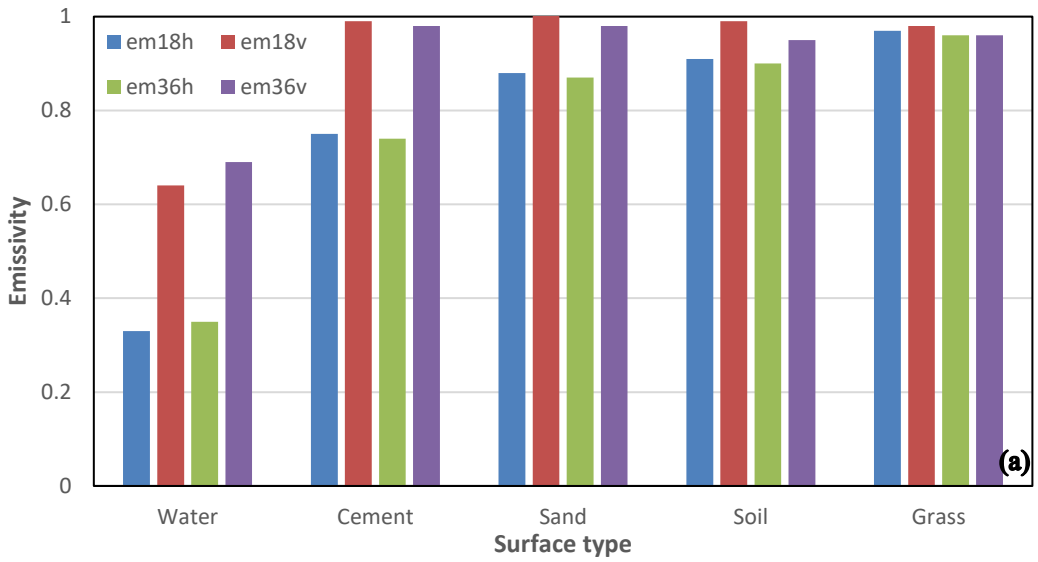

393

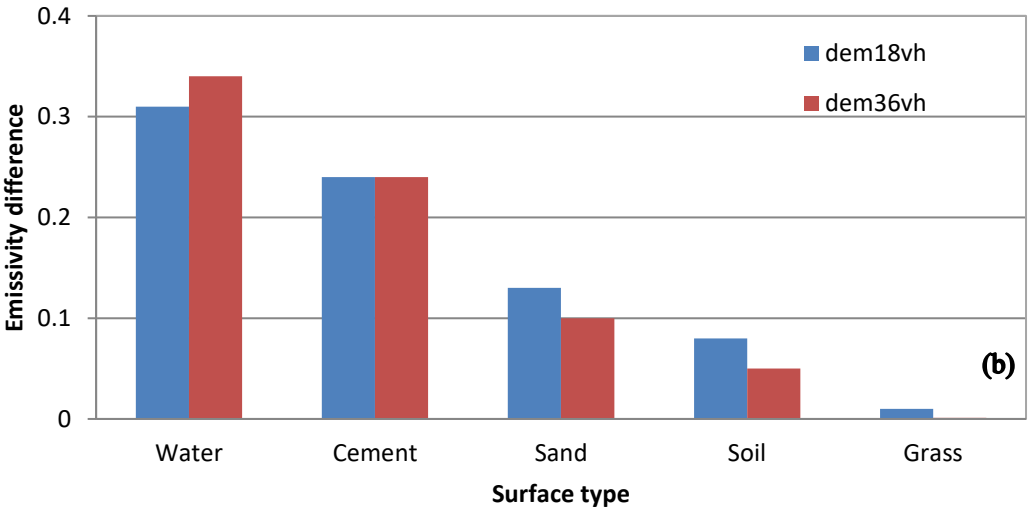

394

395 Fig. 7 Variations in the surface emissivity(a) and emissivity polarization

396 differences (b) over different land surfaces at 02:00 (BJT) in Oct. 2018.

397 In addition to investigating the variations at a fixed angle, the variations in ε at

398 multiple elevation angles over the 4 land surfaces are compared in Fig. 8a. Because ε_h

399 is more sensitive to surface type than to water, when the elevation angle changes from

400 -24° to 65°, ε_h clearly rises from 0.65 to 0.85 over cement, followed by sand and bare

401 soil with ε_h increasing from 0.85 to 0.95, and ε_h is constant at 0.95 over grass. The

402 corresponding ε_v values over the four land surfaces are closer and exhibit a slightly

403 decreasing trend within the range of 0.9-1.0 with increasing elevation angle.

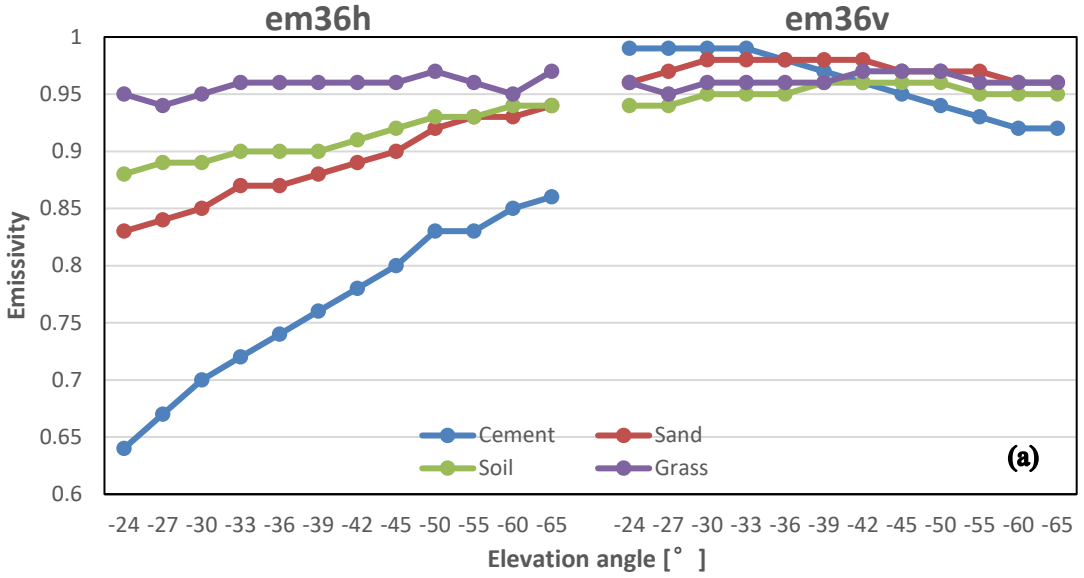

404

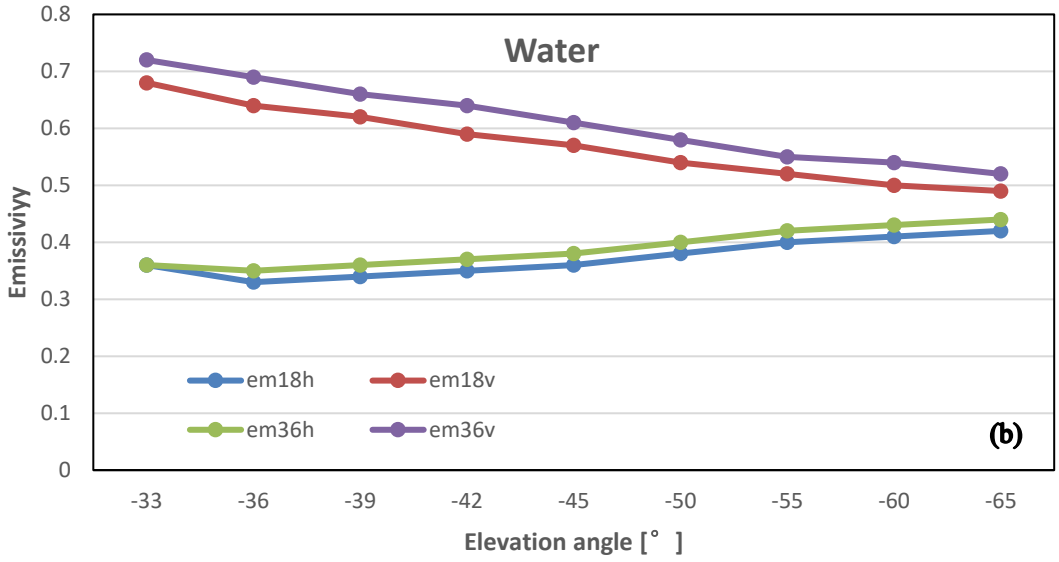

405

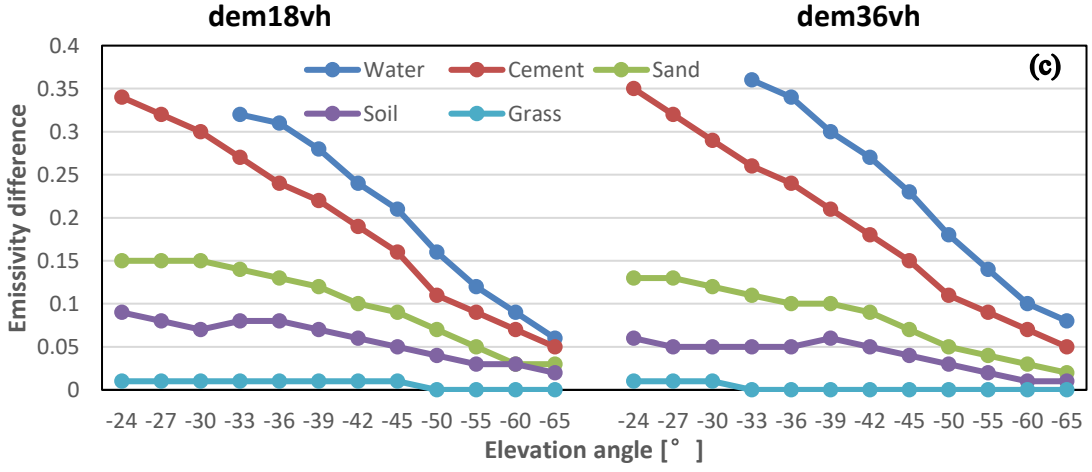

406

407 Fig. 8 Variations in the surface emissivity (a, b) and ε polarization

408 differences(c) over different surfaces with increasing elevation angle in Oct. 2018.

Differ from land surfaces, the ε values over water in Fig. 8b show considerably different variation trends with the elevation angle: when the elevation angle changes from -33° to -65°, ε_v clearly reduces from 0.7 to 0.5, while ε_h slightly increases within the vicinity of 0.4. The corresponding ε polarization differences (ε_v-ε_h) over 5 surfaces (Fig. 8c) present decreasing trend with increasing elevation angle, and the larger the ε polarization difference in Fig. 7b is, the greater the variation with the elevation angle in Fig. 8c is, i.e. the decreasing trend is most obvious over water and smooth cement, but slightly changes over grass with increasing elevation angle. The variation in the ε polarization difference at 36.5 GHz with the elevation angle is similar to that at 18.75 GHz over all 5 test plots (results not shown).

5 Summary

In this paper, we introduce a ground mobile observation system for directly obtaining surface microwave emissivity estimates over five types of surfaces: water, cement, sand, soil and grass. The mobile observation system consists mainly of a dual-polarized ground-based microwave radiometer, a mobile platform, and auxiliary sensors, and the observation field comprises 5 test plots.

Based on the observed data from the mobile system, we preliminarily investigated the variation characteristics of the surface microwave emissivity over the five different land surfaces. The results show that the horizontally polarized emissivity is more sensitive to land surfaces type than is the vertically polarized emissivity: the former decreases to 0.75 over cement and increases to 0.90 over sand and bare soil and up to 0.97 over grass. The observed polarization difference is

obvious over water (>0.3) and cement (approximately 0.25) but reduces to 0.1 over sand and 0.05 over bare soil and almost 0.01 or close to zero over grass; this trend is similar to that of the Tb polarization difference. For different elevation angles, the horizontally/vertically polarized emissivities over the land surfaces obviously increase/slightly decrease with increasing elevation angle but exhibit the opposite trend over water. The emissivity polarization difference decreases with increasing elevation angle, and the larger the emissivity polarization difference is over a certain surface, the greater the variation with the elevation angle.

We developed a ground mobile observation system for measuring the microwave emissivity over multiple surfaces, and the system has worked stably since September 2018. The preliminary results from our observation system partly reflect similar variation trends to those reported by previous surface emissivity experiments, and some are more related to the variation in emissivity at different elevation angles. In future research, we will carry out further analyses and refine the emissivity parameterization scheme for given surfaces based on long-term observations.

Acknowledgments

This work was supported by National Natural Science Foundation of China [No. 41575033] and National Key Research and Development Program of China [2017YFC1501700]. We thank the staffs at Xianghe site for their maintenance work on microwave radiometer and the ground mobile observation system.

References

Calvet, J. C., Wigneron J. P., Chanzy. A.,Raju S., and Laguerre L.: Microwave dielectric proporeties of a silt-loam at high frequencies, IEEE Trans. Geosci. Remote sensing, 33, 634-642,doi: 10.1109/36.387579, 1995.

457 Fung A. K.: Microwave Scattering and Emission Models and Their Applications. Norwood, MA:
458 Artech House, 1994.
459 Karbou, F., Aires F., Prigent C., and Eymard L.: Potential of Advanced Microwave Sounding Unit-A
460 (AMSU-A) and AMSU-B measurements for atmospheric temperature and humidity profiling over
461 land, Journal of Geophysical Research, 110, D07109, doi:10.1029/2004JD005318, 2005.
462 Hewison T. J.: Airborne measurements of forest and agricultural land surface emissivity at
463 millimeter wavelengths. IEEE Trans. Geosci. Remote sensing., 39, 393-400,
464 DOI:10.1109/36.905247, 2001.
465 Hewison, T. J., and English S. J.: Airborne retrievals of snow and ice surface emissivity at
466 millimeter wavelengths. *IEEE Trans. Geosci. Remote Sens.*, 37, 1871-1887,
467 doi:10.1109/36.774700,1999.
468 Isaacs R. G., Jin Y. Q., Worsham R. D., Deblonde, G., Falcone, V. J.: The RADTRAN microwave
469 surface emission models. IEEE Trans.Geosci. Remote sensing, 27, 433-440,
470 DOI:10.1109/36.29563,1989.
471 Jones, A.S., Vonder Haar, T.H.: Retrieval of microwave surface emittance over land using
472 coincident microwave and infrared satellite measurements，*J. Geophys. Res.*,102,13,609-13,626,
473 https://doi.org/10.1029/97JD00797,1997.
474 Lemmetyinen, J., Derksen C., Toose, P., Proksch,C., Pulliainen, J., Kontu, A., Rautiainen, K.,
475 Seppänen, J., Hallikainen, M.: Simulating seasonally and spatially varying snow cover brightness
476 temperature using HUT snow emission model and retrieval of a microwave effective grain size,
477 Remote Sens. Environ.,156,71-95, http://dx.doi.org/10.1016/j.rse.2014.09.016,2015.
478 Mazler C.: Seasonal evolution of microwave radiation from an oat field, Remote Sens. Environ., 31,
479 161-173, doi:10.1016/0034-4257(90)90086-2,1990.
480 Mazler C.: Passive microwave signatures of landscapes in winter, Meteorol. Atmos. Phys., 54,
481 241-260, https://doi.org/10.1007/BF01030063, 1994.
482 McNally A. P., Derber J. C., Wu W. S., Katz, B.B.: The use of TOVS level-1B radiances in the
483 NCEP SSI analysis system, Quarterly Journal of the Royal Meteorological Society, 126, 689-724,
484 https://doi.org/10.1002/qj.49712656315, 2000.
485 Mo, T., Schmugge, T.J.: A parameterization of the effect of surface roughness on microwave
486 emission, IEEE Trans. Geosci. Remote Sens., 4, 481–486, **doi:** 10.1109/TGRS.1987.289860,
487 1987.
488 Moncet, J.L., P. Liang, J. F., Galantowicz, et al., 2011: Land surface microwave emissivities derived
489 from AMSR-E and MODIS measurements with advanced quality control. *J. Geophys. Res.*, 116,
490 D16104, doi:10.1029/2010JD015429.
491 Montpetit, B., Royer, A., Roy, A., Langlois, A.: In-situ passive microwave emission model
492 parameterization of sub-arctic frozen organic soils, Remote Sens. Environ.,205,112-118,
493 https://doi.org/10.1016/j.rse.2017.10.033,2018.
494 Morland, J. C., Grimes D.I.F., Dugdale, G., Hewison, T.J.: The Estimation of Land Surface
495 Emissivities at 24 GHz to 157 GHz Using Remotely Sensed Aircraft Data, Remote Sens. Environ.,
496 73, 323-336, https://doi.org/10.1016/S0034-4257(00)00108-5,2000.
497 Morland, J. C., Metcalfe J., and Walker A.: Microwave remote sensing of soil moisture in southern
498 Ontario: Aircraft and satellite measurements at 19 and 37 GHz, Radio Sci., 38, 8073,
499 doi:10.1029/2002RS002677, 2003.
500 Njoku, E.G., and O'Neill P. E.: Multifrequency microwave radiometer measurements of soil

moisture, IEEE Trans. *Geosc. Remote Sens.,* 20, 468-475, doi:10.1109/TGRS.1982.350412, 1982.
Ruston R. C., Vonder Haar T. H.: Characterization of summertime microwave emissivity from the Special Sensor Microwave Imager over the conterminous United States, J. Geophys. Res., 109, D19103, doi:10.1029/2004JD004890, 2004.
Prigent，C., Rossow, W.B., Matthews, E.:Microwave land surface emissivities estimated from SSM/I observations, *J. Geophys. Res.*,102, 21867-21890, https://doi.org/10.1029/97JD01360,1997.
Prigent, C., Rossow, W. B., Matthews, E., and Marticorena, B.: Microwave radiometric signatures of different surface types in deserts, *Journal of Geophysical Research*, 104, 12147-12158, doi: 10.1029/1999JD900153, doi:10.1029/1999JD900153, 1999.
Prigent, C., Wigneron, J. P., Rossow, W. B., and Pardo-Carrionet, J.R.: Frequency and angular variations of land surface microwave emissivities: Can we estimate SSM/T and AMSU emissivities from SSM/I emissivities? IEEE Trans.Geosci. Remote sensing, 38, 2373-2386, doi:10.1109/36.868893, 2000.
Prigent, C., Aires F., and Rossow W. B.: Land surface microwave emissivities over the globe for a decade, Bull. Amer. Meteorol. Soc., 87, 1573 - 1584, https://doi.org/10.1175/BAMS-87-11-1573, 2006.
Schwartz, C. S., Liu, Z. Q., Chen, Y., Huang, X.Y.: Impact of assimilating microwave radiances with a limited-area ensemble data assimilation system on forecasts of Typhoon Morakot, Weather Forecasting, 27, 424-437, https://doi.org/10.1175/WAF-D-11-00033.1,2012.
Ulaby, F. T., Moore, R. K., Fung, A. K.: Microwave Remote Sensing: Active and Passive. Vol. 3: From Theory Applications. Addison-Wesley Publ. Company, Readings, Massachusettes, 1986.
Wang, J. R. and Choudhury, B. J.: Remote sensing of soil moisture content over bare field at 1.4 GHz frequency, J. Geophys. Res., 86, 5277–5282, 1981.
Wigneron, J. P., Guyon, D., Calvet, J. C., Courrieer G., Bruguier N.: Monitoring coniferous forest characteristics using a multifrequency microwave radiometry, Remote Sens. Environ., 60, 299-310, doi:10.1016/S0034-4257(96)00212-X,1997.
Weng, F., Yan, B., Grody N.C.: A microwave land emissivity model, J. Geophys. Res., 106, 20,115-20,123, https://doi.org/10.1029/2001JD900019, 2001.
Xie, Y., Shi, J., Ji, D., Zhong, J., Fan, S.：A Parameterized Microwave Emissivity Model for Bare Soil Surfaces，Remote sensing, 9, 155-170, https://doi.org/10.3390/rs9020155, 2017.